Single-molecule studies of fork dynamics in Escherichia coli DNA replication

Tanner, Nathan A.; Hamdan, Samir M.; Jergic, Slobodan; Loscha, Karin V.; Schaeffer, Patrick M.; Dixon, Nicholas E.; Oijen, Antoine M. van

Published in:
Nature Structural & Molecular Biology

DOI:
10.1038/nsmb0908-998a

Publication date:
2008

nature structural & molecular biology

Single-molecule studies of fork dynamics in *Escherichia coli* DNA replication

Nathan A Tanner[1,2], Samir M Hamdan[1], Slobodan Jergic[3,4], Karin V Loscha[3], Patrick M Schaeffer[3,5], Nicholas E Dixon[3,4] & Antoine M van Oijen[1]

We present single-molecule studies of the *Escherichia coli* replication machinery. We visualize individual *E. coli* DNA polymerase III (Pol III) holoenzymes engaging in primer extension and leading-strand synthesis. When coupled to the replicative helicase DnaB, Pol III mediates leading-strand synthesis with a processivity of 10.5 kilobases (kb), eight-fold higher than that by Pol III alone. Addition of the primase DnaG causes a three-fold reduction in the processivity of leading-strand synthesis, an effect dependent upon the DnaB-DnaG protein-protein interaction rather than primase activity. A single-molecule analysis of the replication kinetics with varying DnaG concentrations indicates that a cooperative binding of two or three DnaG monomers to DnaB halts synthesis. Modulation of DnaB helicase activity through the interaction with DnaG suggests a mechanism that prevents leading-strand synthesis from outpacing lagging-strand synthesis during slow primer synthesis on the lagging strand.

Complete and accurate replication of DNA involves the coordinated activity of many proteins. The replisome, the molecular machinery of DNA replication, unwinds the double-stranded DNA (dsDNA), synthesizes primers to initiate synthesis and polymerizes nucleotides onto each of the two growing strands[1]. The remarkably efficient replication system of *Escherichia coli* is ideal for studying the dynamic interplay among the various components at the replication fork[1,2]. A fully functional replisome can be reconstituted *in vitro* with a limited number of purified key protein components: the DnaB helicase unwinds dsDNA; the DnaG primase synthesizes short oligoribonucleotides for priming of synthesis of the lagging strand; and the DNA polymerase III (Pol III) holoenzyme polymerizes nucleotides onto each nascent strand[1,3] (**Fig. 1**).

The Pol III holoenzyme is composed of three subassemblies: a core polymerase, a sliding clamp and a clamp-loading complex. The core is a heterotrimer of three subunits: α, the DNA polymerase; ε, a proofreading exonuclease; and θ, which stabilizes ε[4]. The αεθ core is a poorly processive polymerase that incorporates <20 nucleotides before dissociating from the primer-template[5]. However, when tethered to the sliding clamp, a ring-shaped homodimer of β subunits that encircles dsDNA, the processivity of the core increases markedly to several kilobases (kb) at $\sim$750 base pairs (bp) s^{-1} (ref. 5). The loading of the β_2 clamp onto the primer-template strand requires opening of the ring by the γ multiprotein clamp-loading complex[6]. The γ complex contains up to six different subunits required for clamp loading and coordination of the different enzymatic activities at the fork. A minimal γ complex that supports clamp loading contains three copies of the γ protein and one copy each of δ and δ′ (ref. 7). To tether the clamp loader to the dual polymerases at the fork, two γ subunits in the clamp-loading complex are replaced by τ. γ and τ are products of the same gene, *dnaX*, with γ being smaller by 34 kDa in the C-terminal region owing to a programmed frameshift[8]. It is this C-terminal bridge domain of τ that is responsible for core-τ and τ-DnaB interactions[9,10] (**Fig. 1**). Both τ and γ hydrolyze ATP and bind δ and δ′, modulating binding and opening of β_2 (ref. 7,11). Additionally, χ and ψ proteins associate with the γ complex to allow recognition of the single-stranded DNA (ssDNA) binding protein SSB to facilitate lagging-strand primase-polymerase switching[12,13].

The DnaB helicase is a hexameric ATPase that is loaded onto ssDNA by DnaC and the primosomal proteins[14]. DnaB encircles the lagging strand and translocates toward the fork in the 5′ to 3′ direction, thereby displacing the complementary leading strand. DnaB catalyzes unwinding with poor processivity, but in the context of the replisome a single DnaB hexamer supports extensive synthesis of tens of kilobases[15,16]. Serving as the central anchoring component of the replisome, DnaB couples polymerase activity to fork propagation through τ-DnaB interaction and also binds the DnaG primase to regulate the production and deposition of primers on the lagging strand[17]. DnaG alone catalyzes the synthesis of 'overlong' ribonucleotide primers at an approximate rate of one primer every 1,000 s—insufficient for proper replisome function[18]. Much like those of the other replisomal components, its efficiency increases considerably in the presence of the other replication proteins. When DnaG is bound to DnaB, DnaG priming efficiency increases 1,000-fold, synthesizing a primer

[1]Department of Biological Chemistry and Molecular Pharmacology and [2]Graduate Program in Biological and Biomedical Sciences, Harvard Medical School, 250 Longwood Avenue, Boston, Massachusetts 02115, USA. [3]Research School of Chemistry, Australian National University, Canberra, Australian Capital Territory 0200, Australia. [4]School of Chemistry, Building 18, Northfields Avenue, University of Wollongong, New South Wales 2522, Australia. [5]School of Pharmacy and Molecular Sciences, James Cook University, Townsville, Queensland 4811, Australia. Correspondence should be addressed to A.M.v.O. (antoine_van_oijen@hms.harvard.edu).

Received 13 September 2007; accepted 3 January 2008; published online 27 January 2008; corrected after print 18 June 2008; doi:10.1038/nsmb.1381

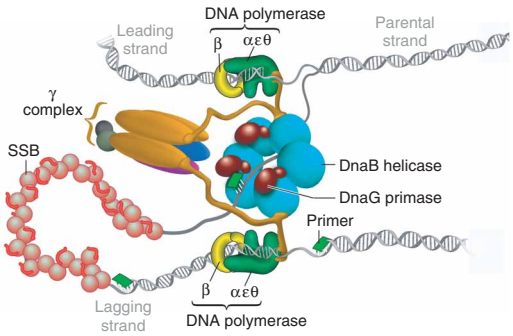

Figure 1 Schematic representation of the *E. coli* replisome mediating coordinated DNA synthesis. Three DnaG primase monomers are shown interacting with the DnaB helicase, adding an RNA primer (green) onto the single-stranded DNA binding protein (SSB)-coated lagging strand.

every 1–2 s, which results in a deposition of primers onto the lagging strand at ~1–2-kb intervals[19–21].

As many as three DnaG monomers bind to a DnaB hexamer[21]. Several models have been posited to explain this stoichiometry and its functional relevance to replisome activity. Many structural and biochemical studies suggest that interactions between adjacent DnaG subunits docked to the DnaB hexamer regulate primase activity, although no definitive picture has emerged[22,23]. To understand how the DnaG-DnaB interaction modulates replisome dynamics requires a kinetic and quantitative characterization of the many transient intermediates involved in replication. With the ensemble averaging inherent in bulk biochemical methods, a population of reactions loses its synchronicity quickly after initiation of the reaction. This dephasing makes observation of any intermediates that occur during replication challenging. Recent advances in imaging and molecular manipulation techniques have made it possible to observe individual proteins and record 'molecular movies' that provide new insight into protein dynamics and reaction mechanisms[24,25]. Here we report the use of single-molecule techniques to observe, in real time, the replication of individual DNA molecules by the *E. coli* replication machinery, thereby substantially extending the reach of *in vitro* single-molecule methods to the study of large (>10 proteins, >1 MDa) multiprotein complexes. The results detailed here suggest that the cooperative binding of three DnaG subunits to a DnaB hexamer destabilizes the replication fork. This modulation of leading-strand replication through the interaction of primase with DnaB suggests a mechanism that prevents leading-strand synthesis from outpacing lagging-strand replication during slow primer synthesis on the lagging strand.

RESULTS

Single-molecule experimental design

We characterized the kinetics of replication reactions at the single-molecule level by stretching individual DNA molecules and monitoring their lengths in the presence of various *E. coli* replication proteins. The 5′ end of one strand of a 48.5-kb duplex λ phage DNA molecule was attached to the bottom surface of a glass flow cell via a biotin-streptavidin linker. The opposite 3′ end was linked using a digoxigenin–anti-digoxigenin interaction to a 2.8-μm-diameter bead (**Fig. 2a**). When a laminar flow was applied above the surface, a force proportional to the flow rate and the diameter of the polymer bead stretched the DNA molecules (**Fig. 2b**). We measured changes in the lengths of the individual DNA molecules by imaging the beads and tracking their positions. An intrinsic structural property of DNA is that ssDNA is substantially shorter than dsDNA at forces lower than 6 pN[26–28] (**Fig. 2c**). As a consequence, conversion from dsDNA to ssDNA can be monitored through a decrease in total DNA length. Conversely, the production of dsDNA from an ssDNA template will result in a net lengthening of the polymer. We used these well-defined differences in length to characterize the activity of enzymes that convert one form of DNA into the other[26,27,29–31].

Pol III holoenzyme extends primers in short steps

To demonstrate the effectiveness of DNA length measurements as an activity probe for *E. coli* replication proteins, we studied DNA synthesis by individual Pol III holoenzymes. Polymerase activity can be visualized by attaching ssDNA molecules between the glass surface and the bead (**Fig. 3a**). To prepare ssDNA, we treated surface-attached dsDNA *in situ* with the replication proteins of bacteriophage T7, which catalyze extensive strand-displacement synthesis on our substrate[29]. After conversion of long stretches of dsDNA into ssDNA, the flow cell was washed extensively to remove excess proteins, and a 30-nt DNA primer was introduced to anneal to the surface-attached ssDNA (**Fig. 3a**). *E. coli* Pol III holoenzyme was reconstituted in the flow cell by introduction of $\tau_2\gamma_1\delta\delta'$, $\alpha\varepsilon\theta$ and β_2 at equimolar (30 nM) concentrations, together with the necessary ATP and dNTPs (for protein purification and reconstitution information, see **Supplementary Figs. 1–3** online). The positions of DNA-attached beads were recorded on a CCD camera during primer extension by the Pol III holoenzyme and tracked over the course of the experiment. Bead position was then plotted versus time to generate single-molecule trajectories of enzymatic activity (**Fig. 3b** and **Supplementary Fig. 4** online).

Template-directed nucleotide incorporation at the 3′ terminus of the primer converts ssDNA to dsDNA, and this process was observed as a lengthening of the DNA. The presence of a low concentration of holoenzyme in solution (30 nM) gave rise to short bursts of enzymatic activity, corresponding to repeated cycles of single extension events: association of the polymerase with the DNA; processive synthesis; and polymerase dissociation from the DNA primer-template (**Fig. 3b**). No

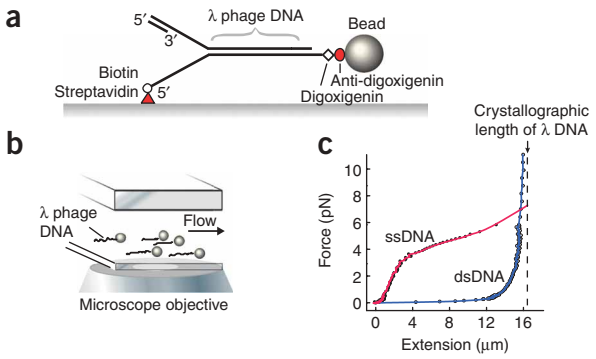

Figure 2 Single-molecule experimental setup. (**a**) Duplex λ DNA (48.5 kb) was attached to the surface of the flow cell via the 5′ end of the fork using a biotin-streptavidin interaction, and the 3′ end was attached to a bead using a digoxigenin–anti-digoxigenin interaction. A primed replication fork was formed at the end opposite the bead to allow loading and initiation of the replication proteins. (**b**) Bead-DNA assemblies were stretched using laminar flow of buffer and imaged using wide-field optical microscopy, permitting simultaneous observation of multiple individual replication reactions. (**c**) Extension profile of single-stranded DNA (ssDNA; filled circle) and double-stranded DNA (dsDNA; open circle) under low forces. The dashed line shows the crystallographic length of fully ds-λ DNA, 16.3 μm[29].

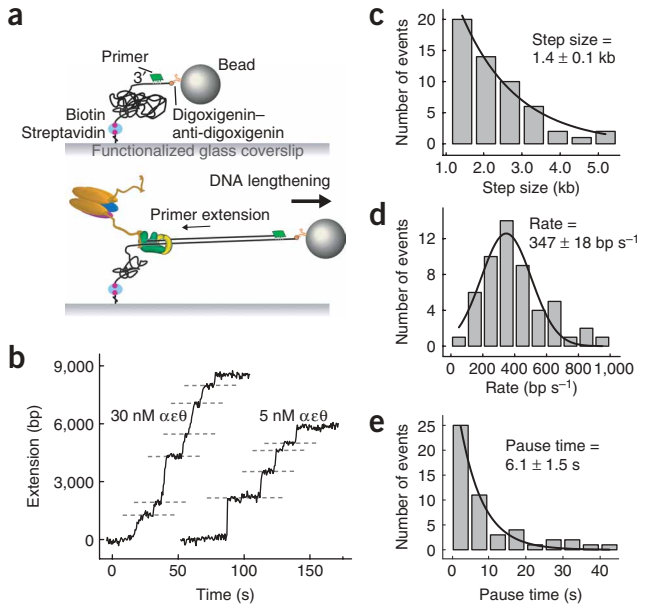

Figure 3 Primer extension by the DNA polymerase III holoenzyme. (**a**) ssDNA was generated in the flow cell and an oligonucleotide primer was annealed (see text). Proteins were introduced with dNTPs and ATP, and primer-extension activity was measured as a lengthening of the tethered DNA. (**b**) Examples of lengthening traces, with extension at 30 nM αεθ on the left and 5 nM αεθ on the right. Dashed lines represent points where pauses in the DNA extension were identified. (**c**) Distribution of lengthening step sizes, fit with a single-exponential decay. (**d**) Distribution of rates, fit with a Gaussian distribution. (**e**) Distribution of lengths of pauses between lengthening steps, fit with a single-exponential decay. Data shown are from experiments carried out with 30 nM Pol III holoenzyme.

length change was observed in the absence of dNTPs or with the αεθ core polymerase alone. The height of the individual steps is a measure of processivity and obeys a single-exponential distribution with a decay constant of 1.4 ± 0.1 kb (**Fig. 3c**). The single-exponential nature of the processivity distribution is consistent with a single rate constant determining the kinetics of the enzyme dissociating from the primer-template DNA[32]. The slopes of the DNA lengthening steps report the instantaneous polymerization rate and show a distribution with a mean of 347 ± 18 bp s^{-1} (**Fig. 3d**). Repeating the experiment with a limiting concentration of αεθ (5 nM) resulted in identical step sizes (1.3 ± 0.3 kb) and rates (505 ± 26 bp s^{-1}), but an increased pause time between steps, from 6.1 ± 1.5 s at 30 nM αεθ to 21.1 ± 2.6 s at 5 nM (**Fig. 3b,e** and **Supplementary Fig. 5** online). This increase reflects the lower association rate of the holoenzyme with the primer at the lower protein concentration and confirms that the observed lengthening steps are indeed true single-enzyme events.

Early bulk-phase biochemical studies demonstrated a processivity of the Pol III holoenzyme of 100 to several hundreds of nucleotides in the absence of SSB, although it has been difficult to obtain precise values[5]. The use of ensemble-averaging techniques to measure processivity values is often complicated by the occurrence of multiple consecutive events of binding, synthesis and dissociation on one and the same DNA molecule, a situation that is difficult to distinguish from a single highly processive event. The real-time observation of primer extension by individual Pol III holoenzymes provides direct information on polymerization kinetics with increased quantitative precision.

E. coli leading-strand synthesis is highly processive

Next, we examined DNA replication by Pol III together with DnaB. By flowing the Pol III holoenzyme and DnaB into the flow cell, we were able to initiate leading-strand synthesis on tethered λ dsDNA containing a premade replication fork (**Fig. 4a**). To facilitate loading of the hexameric DnaB onto the premade fork, we included the DnaB loader protein DnaC[33]. DNA synthesis catalyzed by the Pol III holoenzyme converts the ssDNA arising from DnaB helicase activity into dsDNA. To restrict replicative activity to the leading strand, we used a clamp-loading complex of stoichiometry $\tau_1\gamma_2\delta\delta'$, allowing the assembly of only one Pol III core[34]. In addition, the absence of χ and ψ from the clamp-loading complex, and the omission of DnaG and SSB, assure the preclusion of lagging-strand synthesis. Proteins were introduced at equimolar concentrations into a flow chamber heated to 37 °C, with ATP and dNTPs. In the presence of leading-strand synthesis and absence of lagging-strand synthesis, the leading strand was converted into dsDNA whereas the lagging strand remained in the single-stranded form. By attaching the DNA to the surface of the flow cell by the 5′ biotin-labeled lagging strand, leading-strand synthesis was detected by an effective shortening of the DNA (**Fig. 4a**).

Leading-strand synthesis was observed as highly processive DNA-shortening events (**Fig. 4b** and **Supplementary Fig. 6** online). No change in DNA length was seen when the experiment was carried out without dNTPs or with only the Pol III holoenzyme, which is not capable of strand-invasion synthesis[9]. Furthermore, no DNA length change was observed in the presence of only DnaB and its loader DnaC, which is consistent with the inability of the DnaB helicase to unwind stretches of dsDNA longer than 30 bp in bulk-phase experiments[15]. The interaction between DnaB and τ is thought to increase helicase processivity[9]. However, when DnaBC and either the $\tau_1\gamma_2\delta\delta'$ or the $\tau_2\gamma_1\delta\delta'\chi\psi$ complex were added to the flow cell and the Pol III

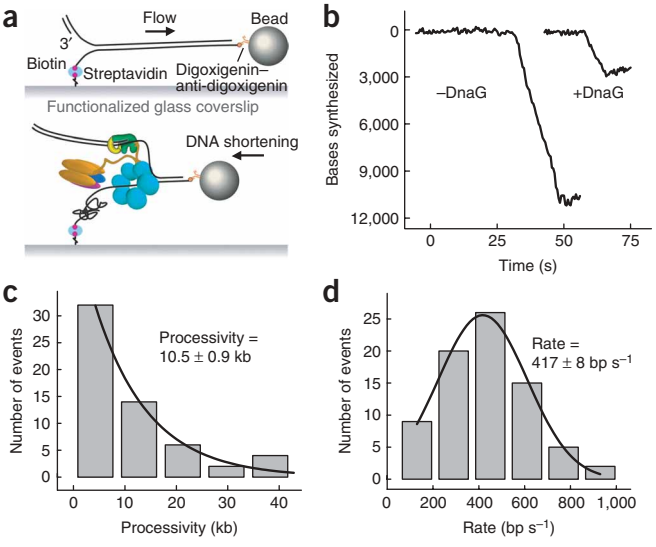

Figure 4 Leading-strand synthesis by Pol III holoenzyme coupled with DnaB helicase. (**a**) Duplex λ DNA with a pre-made replication fork was stretched under laminar flow, and Pol III holoenzyme, DnaB and DnaC were introduced into the chamber. Synthesis was observed as a shortening of the tethered DNA. (**b**) Examples of leading-strand synthesis traces, in the absence (left) and presence (right) of DnaG. (**c**) Distribution of leading-strand synthesis processivities, fit with a single-exponential decay. Leading-strand synthesis was observed as single shortening events with an average processivity of 10.5 kb. (**d**) Distribution of synthesis rates, fit with a Gaussian distribution.

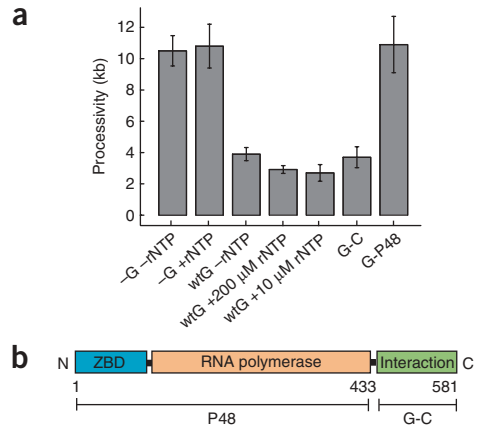

Figure 5 Replicative abortion is independent of DnaG primase activity. (**a**) Processivities of leading-strand synthesis as obtained from single-molecule experiments under indicated conditions. (**b**) DnaG is composed of three major domains: zinc binding (ZBD), the RNA polymerase and DnaB-interaction domains. Mutant DnaG-P48 is a deletion of the C-terminal 148-residue interaction domain, and G-C is a deletion of the N-terminal 433-residue primase domains, as indicated by the brackets.

holoenzyme was omitted from the reaction, no DNA length change could be seen (**Supplementary Fig. 6**). We therefore conclude that our observation of DNA shortening is due to DNA synthesis activity of a single *E. coli* leading-strand synthesis complex.

Analysis of 65 individual leading-strand synthesis reactions resulted in a measured processivity of 10.5 ± 0.9 kb and a mean synthesis rate of 417 ± 8 bp s^{-1} (**Fig. 4c,d**). This processivity value was lower than expected based on previously reported bulk-phase biochemical studies, which determined the processivity of the Pol III holoenzyme complexed to DnaB to be >50 kb[16]. A possible explanation is that the single-molecule experiments allow for an unequivocal discrimination between one processive event and multiple successive ones. The length of final DNA products as observed in bulk-phase experiments could result from multiple synthesis events on an individual DNA molecule. Also, the topological challenge faced by DnaB to assemble on the surface-immobilized 5′ terminus of the premade fork in our experiments could result in a lower probability of reinitiation of leading-strand synthesis after dissociation of one of the components from the primer template. Consistent with previous observations that χ and ψ function outside of leading-strand synthesis[13], we found that the processivity and rate values are similar for reactions carried out with the $\tau_2\gamma_1\delta\delta'$ (8.5 ± 2.4 kb at 380 ± 51 bp s^{-1}) or the $\tau_2\gamma_1\delta\delta'\chi\psi$ (7.5 ± 2.8 kb at 300 ± 73 bp s^{-1}) clamp-loading complexes. The force used in this experiment acts to stretch the DNA but is sufficiently low as to not affect local DNA-protein or base pair interactions[35]. As a control, reducing the DNA-stretching force from 3 pN to 1 pN resulted in similar rates and processivities (7.4 ± 0.3 kb at 528 ± 133 bp s^{-1}). We therefore concluded that our experimentally observed values are accurate measures of single Pol III–DnaB leading-strand synthesis events.

DnaG binding to DnaB destabilizes the replisome

We next aimed to examine the effects of DnaG primase activity on leading-strand synthesis. Earlier single-molecule experiments on the bacteriophage T7 replication system revealed that primase activity resulted in pausing of leading-strand synthesis[29]. However, with the *E. coli* system, the addition of DnaG (300 nM) and rNTPs (200 μM each) to the leading-strand synthesis reactions resulted in a drastic reduction of the processivity, and no discrete pausing events were observed (**Fig. 4b** and **Supplementary Fig. 6**). On average, the replication reaction stopped after synthesis of 2.9 ± 0.5 kb. The rate of leading-strand synthesis (340 ± 28 bp s^{-1}) was similar to that obtained in the absence of primase activity. Adding only rNTPs without DnaG did not result in a reduction of the processivity (10.8 ± 1.4 kb), indicating that the lower processivity of leading-strand synthesis observed with DnaG was not due to rNTPs affecting polymerase activity (**Fig. 5a**).

Next, we sought to examine more fully the effects of the two aspects of DnaG function, primer synthesis and DnaG-DnaB interaction, in causing shortening of leading-strand synthesis. To reduce or inhibit primase activity while allowing DnaG to interact with DnaB, we carried out the experiment both with a decreased rNTP concentration and without rNTPs entirely. We observed consistently decreased processivities of 2.7 ± 0.5 kb and 3.9 ± 1 kb respectively, indicating that fork stalling is independent of rNTP concentration (**Fig. 5a**). Additionally, we repeated the experiments using a truncated DnaG that lacks the C-terminal 16-kDa domain responsible for interaction with DnaB, but retains full primase activity (DnaG-P48)[36,37] (**Fig. 5b**). We observed a high processivity value (10.9 ± 1.8 kb), indicating that DnaG-DnaB interactions are necessary to cause replicative stall (**Fig. 5a**). These results suggest that reduced processivity of leading-strand synthesis is independent of primer synthesis.

To determine whether DnaG-DnaB interactions are indeed sufficient to modulate leading-strand synthesis, we introduced a truncated DnaG comprising only the 148-residue domain responsible for interaction with DnaB (DnaG-C)[37] (**Fig. 5b**). In the presence of 300 nM DnaG-C, the processivity of leading-strand synthesis was measured to be 3.6 ± 0.5 kb, consistent with the value measured with the full-length primase (**Fig. 5a**). In summary, these results indicate that the DnaG-DnaB interaction is the cause of premature abortion of leading-strand synthesis in the presence of DnaG.

Cooperative DnaG-DnaB interactions destabilize the replisome

Previous studies have shown that up to three DnaG monomers can bind to a single DnaB hexamer[21,37,38]. Models involving interactions between adjacent DnaB-bound DnaG monomers have been proposed as possible mechanisms of regulating primase activity[22,23]. To investigate the effect of DnaG oligomerization on replication fork progression, we carried out the single-molecule leading-strand synthesis experiment with various concentrations of DnaG in the presence of rNTPs (200 μM each) and measured the processivity of leading-strand synthesis (**Fig. 6**, squares). Fitting the processivities with a cooperative binding equation (**Fig. 6**, dashed line) resulted in a Hill coefficient of 2.6, suggesting that cooperative binding of two or three DnaG molecules to the DnaB hexamer leads to a reduced processivity of the replisome. This cooperativity is different from earlier equilibrium binding studies of the interaction between DnaG and DnaB, which observed a non-cooperative interaction[37]. Furthermore, we determined an effective K_D of 50 ± 6 nM, substantially lower than the K_D of ~2 μM obtained from previously published binding studies[37].

DnaG N-terminus is needed for cooperative DnaG-DnaB interaction

Although high concentrations of the DnaG mutant containing only the DnaB interaction domain (DnaG-C, **Fig. 5b**) result in a reduced processivity, it is not clear whether DnaB-DnaG interactions are

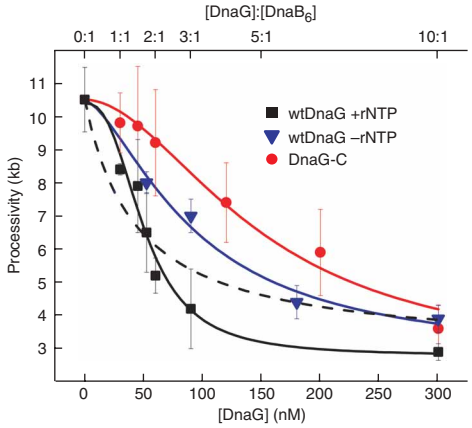

Figure 6 Cooperative DnaG-DnaB interaction is dependent upon the RNA polymerase domain of primase. Processivity values for increasing concentrations of wild-type DnaG (wtDnaG) with rNTPs (squares), of wtDnaG without rNTPs (triangles) and of the mutant DnaG-C (with a deletion of the C-terminal 148-residue interaction domain) without rNTPs (circles). The DnaG concentration and DnaG:$DnaB_6$ concentration ratio in solution is indicated at the bottom and top axis, respectively. Data are fit with the binding equation $y = \frac{[\text{DnaG}]^h}{[\text{DnaG}]^h + K_D^h} \times A + B$, where h is the Hill coefficient, and A and B are scaling parameters. Fit lines are shown for each condition: DnaG +rNTPs (black; $K_D = 50.7 \pm 5.8$, $h = 2.6 \pm 0.8$), DnaG –rNTPs (blue; $K_D = 93 \pm 40$, $h = 1.5 \pm 0.8$) and DnaG-C (red; $K_D = 150 \pm 9$, $h = 1.8 \pm 0.2$). The dashed line represents a fit to the data obtained with DnaG and rNTPs, fit with the Hill coefficient h held fixed at 1. Its poor fitting emphasizes the presence of cooperativity in DnaG-DnaB binding in the presence of ribonucleotides and RNA polymerase domains.

sufficient to mediate the cooperativity that we observed with the wild-type DnaG. By measuring the processivity of leading-strand synthesis with various concentrations of the DnaG-C mutant, we were able to examine the effect of the absence of zinc binding (ZBD) and RNA polymerase (RNAP) domains on cooperativity between DnaG monomers in replication fork destabilization. Previous structural and biochemical work suggested the existence of interactions between the ZBD of one DnaG subunit and the RNAP domain of another. This cross talk between neighboring DnaG monomers while they are bound to a DnaB hexamer is thought to introduce cooperativity and to have a role in primer synthesis[22,23]. **Figure 6** shows a marked decrease in cooperativity over increasing amounts of DnaG-C (circles), with a lower Hill coefficient of 1.8. The curve is also noticeably shifted to the right, corresponding to a three-fold increase in the apparent K_D (150 ± 9 nM for DnaG-C versus 50 ± 6 nM for the full-length DnaG). This is similar to the difference in K_D observed in surface plasmon resonance studies of binding of DnaG and DnaG-C to ssDNA-bound DnaB[37]. The reduced cooperativity of the interaction between DnaG-C and DnaB emphasizes the importance of the ZBD and RNAP domains for the cooperative DnaG-DnaB interaction. To examine whether this effect is dependent on primase activity, we carried out the experiments with full-length DnaG protein in the absence of rNTPs. The resulting curve is similar to that of experiments with DnaG-C, with a Hill coefficient of 1.5 and a K_D of 93 ± 40 nM (**Fig. 6**, triangles), indicating a role for rNTP binding in the cooperative DnaG-DnaB interaction that mediates stalling of the replication fork. Thus, the N-terminal ZBD and RNAP domains as well as binding of rNTP all seem to be important to achieve cooperativity in the interaction between DnaG and DnaB. These results are consistent with models of intermonomer interactions[22,23] between the ZBD and RNAP domains of adjacent DnaG molecules bound to DnaB, identifying a dependence on rNTP binding to allow these cooperative interactions.

DISCUSSION

The *E. coli* replisome has long served as a model for studying the various activities of DNA replication. Although classic studies have elucidated most of the numerous protein functions and interactions, several aspects of the replisome can be addressed only through direct examination of the components and activities of individual complexes. We report here single-molecule studies of functioning *E. coli* replication proteins and demonstrate our ability to quantitatively describe protein-protein interactions in an active replisome. We have demonstrated the importance of two of these interactions for effective replication. The Pol III holoenzyme alone synthesizes approximately 1.4 kb on a ssDNA template and is incapable of strand-invasion synthesis, but when tethered to DnaB a single complex can synthesize stretches of DNA greater than 10 kb by coupling nucleotide polymerization to strand separation and fork propagation. We argue that the processivity of a single DnaB-Pol III holoenzyme leading-strand complex is only 10.5 kb, as varying the clamp-loading complex stoichiometry or the force of the experiment had no effect, and predominantly single shortening-event traces were observed (that is, reinitiation on a synthesized DNA was readily observable but rare).

We observed a reduction in processivity of leading-strand synthesis upon addition of DnaG and ribonucleotides. In previous single-molecule studies on bacteriophage T7 leading-strand synthesis we reported that, during primer synthesis on the lagging strand, leading-strand synthesis pauses[29]. We proposed that this tight coupling serves as a molecular brake that prevents leading-strand synthesis from outpacing lagging-strand synthesis while a primer is being synthesized. However, the experiments described here demonstrate that the addition of the DnaG C-terminal domain, responsible for interaction with DnaB but devoid of primase activity, to the *E. coli* leading-strand synthesis reaction is sufficient to cause abortion of replication. This observation demonstrates that the termination of leading-strand synthesis is solely dependent on the interaction between DnaG and DnaB, and not on the synthesis of a primer. In the presence of primase activity, the interaction between DnaG and DnaB as observed in our single-molecule experiments is highly cooperative, whereas little cooperativity is observed when using the DnaG mutant that is unable to synthesize primers. This observation supports previously proposed interactions between the ZBD and RNAP domains of adjacent DnaB-bound DnaG monomers[22,23]. Crystal structures of *Bacillus stearothermophilus* DnaB and the helicase binding domain of DnaG show three DnaG monomers interacting with a DnaB hexamer in conformations favoring close proximity, supporting the hypothesis that the primase monomers interact *in trans*[38]. These and similar interactions between primase monomers in the T7 replication system have been proposed to serve as a mechanism of regulating primase activity[22,23,39]. Our experiments demonstrate that, although primase activity is not essential for the premature abortion of leading-strand synthesis, it does modulate the kinetics of the fork halting.

If cessation of leading-strand synthesis is not caused by primase activity but solely by the interaction between DnaG and DnaB, then what is the underlying molecular mechanism? The fact that the processivity remains non-zero at high DnaG concentrations (**Fig. 6**) suggests that, after association of a trimer of DnaG to the DnaB, an additional rate-limiting step needs to take place before replication is stopped. The observation that DnaG-DnaB interactions alone, as

opposed to primase activity, are sufficient for this behavior suggests a model in which DnaG destabilizes or stalls the replisome. A possibility is that cooperative binding of DnaG to DnaB during active DNA replication weakens the interaction between τ and DnaB, leading to more rapid disassembly of the replisome and a reduced processivity. From the single-molecule experiments, we obtained an effective K_D of the interaction between DnaG and DnaB that is substantially lower than observed in bulk-phase binding studies (50 nM compared to 2 μM)[37]. This reduction probably reflects the true strength of the DnaB-DnaG interaction in the context of the replisome, where association of DnaB with the τ subunit of Pol III strengthens its interaction with DnaG, whereas simultaneous interaction of two or three DnaG molecules with DnaB weakens its interaction with τ. The primase-mediated reduction in leading-strand processivity in the absence of SSB may indicate a regulatory mechanism to ensure coupling of leading-strand synthesis to the normal sequence of events during primer synthesis on the lagging strand; primase is believed to dissociate promptly from DnaB following primer synthesis by association with SSB flanking the primer terminus[13]. In the persistent absence of SSB and lagging-strand synthesis, leading-strand replication could stall as a result of easier dissociation of the helicase from the polymerase. Future single-molecule studies of replisomes mediating both leading- and lagging-strand synthesis will further probe these and other processes at the replication fork.

METHODS

Replication proteins. Methods for preparation of the following proteins from overproducing strains were essentially as described in previous reports: DnaB helicase and DnaC helicase loader[40], DnaG primase[41], DnaG-P48 and DnaG-C[37], and the Pol III holoenzyme subunits, α, δ and δ′ (ref. 42), ε and θ (ref. 43), β_2 (ref. 44), γ and χ (ref. 45). Subunit ψ was produced using strain BL21(λDE3)/pLysS/pET-ψ and refolded in the presence of χ to form the ψχ complex, essentially as described[46,47]. Plasmid pJC491, which directs overproduction of the τ, but not the γ, subunit[10], was used to produce τ in the *ompT* strain BL21(λDE3)*recA*[48]; purification of τ based on a published method[49] is described in **Supplementary Figure 1**. The αεθ core subassembly was reconstituted by mixing of purified α with excess ε and θ, and αεθ was then purified by chromatography on a column of DEAE-Sephacel (GE Healthcare), as described in **Supplementary Figure 2**. The clamp loader assemblies $\tau_1\gamma_2\delta\delta'$, $\tau_2\gamma_1\delta\delta$ and $\tau_2\gamma_1\delta\delta'\chi\psi$ were reconstituted by sequential mixing of purified subunits and separated by chromatography on a MonoS column (GE Healthcare), using described methods[50] with modifications outlined in **Supplementary Figure 3**.

Single-molecule DNA replication assay. Phage λ DNA molecules were annealed and ligated to modified oligonucleotides to introduce a biotinylated fork on one end of the DNA and a digoxigenin moiety on the other end as described previously[29]. The resulting DNA molecules were attached with the 5′ terminus of the bifurcated end to the streptavidin-coated glass surface of a flow cell and with the 3′ end of the same strand to a 2.8-μm diameter anti-digoxigenin–coated paramagnetic bead (Dynal). To prevent nonspecific interactions between the beads and the surface, a 1.7-pN magnetic force on the bead was applied upward by positioning a permanent magnet above the flow cell. Experiments were done at 37 °C. Beads were imaged with a CCD camera (Q-Imaging Rolexa Fast) at a time resolution of 500 ms, and their positions were determined by particle-tracking software (Semasopht). Traces were corrected for residual instabilities in the flow by subtracting traces corresponding to tethers that were not enzymatically altered, as described previously[29] (**Supplementary Fig. 7** online). Pauses of primer extension were selected as a minimum of five data points (images taken at 2 Hz) with amplitude fluctuations less than three times the s.d. of the noise ($\sigma = 30$ nm). All error bars represent the error in fitting an exponential (processivity and pause time) or Gaussian distribution (rate).

Unless specified otherwise, *E. coli* proteins were introduced as: $\tau_1\gamma_2\delta\delta'$ (15 nM), αεθ (30 nM), β_2 (30 nM), DnaB (30 nM, as a hexamer), DnaC (180 nM, as a monomer) and DnaG (various) in *E. coli* replication buffer (50 mM HEPES-KOH pH 7.9, 12 mM $Mg(OAc)_2$, 80 mM KCl, 0.1 mg ml^{-1} bovine serum albumin with 5 mM DTT, 760 μM dNTPs, 200μM rNTPs if desired and 1 mM ATP added immediately before introduction to the flow cell). All proteins were present continuously during observation of single-molecule replication events.

Note: Supplementary information is available on the Nature Structural & Molecular Biology website.

ACKNOWLEDGMENTS

The authors thank J. Loparo, Harvard Medical School, Boston, for construction of a flow cell heating apparatus and critical reading of the manuscript, and A.Y. Park and M. Mulcair, Australian National University, Canberra, for preparation of several proteins. We thank S. Moskowitz, Advanced Medical Graphics, for illustrations. This work was supported in part by funding from the US National Institutes of Health and National Science Foundation (A.M.v.O.) and by a grant from the Australian Research Council (N.E.D.).

AUTHOR CONTRIBUTIONS

N.A.T. performed single-molecule experiments, interpreted the data and wrote the manuscript; S.M.H. interpreted the data and designed experiments; S.J. and P.M.S. purified all proteins and complexes; N.E.D. designed experiments and wrote the manuscript; A.M.v.O. designed experiments, interpreted data and wrote the manuscript.

Published online at http://www.nature.com/nsmb/
Reprints and permissions information is available online at http://npg.nature.com/reprintsandpermissions

1. Benkovic, S.J., Valentine, A.M. & Salinas, F. Replisome-mediated DNA replication. *Annu. Rev. Biochem.* **70**, 181–208 (2001).
2. Yuzhakov, A., Turner, J. & O'Donnell, M. Replisome assembly reveals the basis for asymmetric function in leading and lagging strand replication. *Cell* **86**, 877–886 (1996).
3. Wu, C.A. *et al.* Coordinated leading- and lagging-strand synthesis at the *Escherichia coli* DNA replication fork. IV. Reconstitution of an asymmetric, dimeric DNA polymerase III holoenzyme. *J. Biol. Chem.* **267**, 4064–4073 (1992).
4. Kelman, Z. & O'Donnell, M. DNA polymerase III holoenzyme: structure and function of a chromosomal replicating machine. *Annu. Rev. Biochem.* **64**, 171–200 (1995).
5. Fay, P.J., Johanson, K.O., McHenry, C.S. & Bambara, R.A. Size classes of products synthesized processively by DNA polymerase III and DNA polymerase III holoenzyme of *Escherichia coli*. *J. Biol. Chem.* **256**, 976–983 (1981).
6. Bloom, L.B. Dynamics of loading the *Escherichia coli* DNA polymerase processivity clamp. *Crit. Rev. Biochem. Mol. Biol.* **41**, 179–208 (2006).
7. Jeruzalmi, D. *et al.* Mechanism of processivity clamp opening by the delta subunit wrench of the clamp loader complex of *E. coli* DNA polymerase III. *Cell* **106**, 417–428 (2001).
8. Tsuchihashi, Z. & Kornberg, A. Translational frameshifting generates the γ subunit of DNA polymerase III holoenzyme. *Proc. Natl. Acad. Sci. USA* **87**, 2516–2520 (1990).
9. Kim, S., Dallmann, H.G., McHenry, C.S. & Marians, K.J. Coupling of a replicative polymerase and helicase: a τ-DnaB interaction mediates rapid replication fork movement. *Cell* **84**, 643–650 (1996).
10. Jergic, S. *et al.* The unstructured C-terminus of the τ subunit of *Escherichia coli* DNA polymerase III holoenzyme is the site of interaction with the α subunit. *Nucleic Acids Res.* **35**, 2813–2824 (2007).
11. Jeruzalmi, D., O'Donnell, M. & Kuriyan, J. Crystal structure of the processivity clamp loader gamma (γ) complex of *E. coli* DNA polymerase III. *Cell* **106**, 429–441 (2001).
12. Glover, B.P. & McHenry, C.S. The χψ subunits of DNA polymerase III holoenzyme bind to single-stranded DNA-binding protein (SSB) and facilitate replication of an SSB-coated template. *J. Biol. Chem.* **273**, 23476–23484 (1998).
13. Yuzhakov, A., Kelman, Z. & O'Donnell, M. Trading places on DNA–a three-point switch underlies primer handoff from primase to the replicative DNA polymerase. *Cell* **96**, 153–163 (1999).
14. Konieczny, I. Strategies for helicase recruitment and loading in bacteria. *EMBO Rep.* **4**, 37–41 (2003).
15. Galletto, R., Jezewska, M.J. & Bujalowski, W. Unzipping mechanism of the double-stranded DNA unwinding by a hexameric helicase: quantitative analysis of the rate of the dsDNA unwinding, processivity and kinetic step-size of the *Escherichia coli* DnaB helicase using rapid quench-flow method. *J. Mol. Biol.* **343**, 83–99 (2004).
16. Mok, M. & Marians, K.J. The *Escherichia coli* preprimosome and DNA B helicase can form replication forks that move at the same rate. *J. Biol. Chem.* **262**, 16644–16654 (1987).
17. Schaeffer, P.M., Headlam, M.J. & Dixon, N.E. Protein–protein interactions in the eubacterial replisome. *IUBMB Life* **57**, 5–12 (2005).
18. Swart, J.R. & Griep, M.A. Primer synthesis kinetics by *Escherichia coli* primase on single-stranded DNA templates. *Biochemistry* **34**, 16097–16106 (1995).

19. Lu, Y.B., Ratnakar, P.V., Mohanty, B.K. & Bastia, D. Direct physical interaction between DnaG primase and DnaB helicase of *Escherichia coli* is necessary for optimal synthesis of primer RNA. *Proc. Natl. Acad. Sci. USA* **93**, 12902–12907 (1996).
20. Johnson, S.K., Bhattacharyya, S. & Griep, M.A. DnaB helicase stimulates primer synthesis activity on short oligonucleotide templates. *Biochemistry* **39**, 736–744 (2000).
21. Mitkova, A.V., Khopde, S.M. & Biswas, S.B. Mechanism and stoichiometry of interaction of DnaG primase with DnaB helicase of *Escherichia coli* in RNA primer synthesis. *J. Biol. Chem.* **278**, 52253–52261 (2003).
22. Corn, J.E., Pease, P.J., Hura, G.L. & Berger, J.M. Crosstalk between primase subunits can act to regulate primer synthesis in trans. *Mol. Cell* **20**, 391–401 (2005).
23. Corn, J.E. & Berger, J.M. Regulation of bacterial priming and daughter strand synthesis through helicase-primase interactions. *Nucleic Acids Res.* **34**, 4082–4088 (2006).
24. Toprak, E. & Selvin, P.R. New fluorescent tools for watching nanometer-scale conformational changes of single molecules. *Annu. Rev. Biophys. Biomol. Struct.* **36**, 349–369 (2007).
25. Greenleaf, W.J., Woodside, M.T. & Block, S.M. High-resolution, single-molecule measurements of biomolecular motion. *Annu. Rev. Biophys. Biomol. Struct.* **36**, 171–190 (2007).
26. Maier, B., Bensimon, D. & Croquette, V. Replication by a single DNA polymerase of a stretched single-stranded DNA. *Proc. Natl. Acad. Sci. USA* **97**, 12002–12007 (2000).
27. Wuite, G.J., Smith, S.B., Young, M., Keller, D. & Bustamante, C. Single-molecule studies of the effect of template tension on T7 DNA polymerase activity. *Nature* **404**, 103–106 (2000).
28. Bustamante, C., Bryant, Z. & Smith, S.B. Ten years of tension: single-molecule DNA mechanics. *Nature* **421**, 423–427 (2003).
29. Lee, J.B. *et al.* DNA primase acts as a molecular brake in DNA replication. *Nature* **439**, 621–624 (2006).
30. van Oijen, A.M. Honey, I shrunk the DNA: DNA length as a probe for nucleic-acid enzyme activity. *Biopolymers* **85**, 144–153 (2007).
31. van Oijen, A.M. *et al.* Single-molecule kinetics of λ exonuclease reveal base dependence and dynamic disorder. *Science* **301**, 1235–1238 (2003).
32. Schnitzer, M.J. & Block, S.M. Statistical kinetics of processive enzymes. *Cold Spring Harb. Symp. Quant. Biol.* **60**, 793–802 (1995).
33. Wahle, E., Lasken, R.S. & Kornberg, A. The dnaB-dnaC replication protein complex of *Escherichia coli*. II. Role of the complex in mobilizing dnaB functions. *J. Biol. Chem.* **264**, 2469–2475 (1989).
34. McInerney, P., Johnson, A., Katz, F. & O'Donnell, M. Characterization of a triple DNA polymerase replisome. *Mol. Cell* **27**, 527–538 (2007).
35. Bustamante, C., Smith, S.B., Liphardt, J. & Smith, D. Single-molecule studies of DNA mechanics. *Curr. Opin. Struct. Biol.* **10**, 279–285 (2000).
36. Tougu, K., Peng, H. & Marians, K.J. Identification of a domain of *Escherichia coli* primase required for functional interaction with the DnaB helicase at the replication fork. *J. Biol. Chem.* **269**, 4675–4682 (1994).
37. Oakley, A.J. *et al.* Crystal and solution structures of the helicase-binding domain of *Escherichia coli* primase. *J. Biol. Chem.* **280**, 11495–11504 (2005).
38. Bailey, S., Eliason, W.K. & Steitz, T.A. Structure of hexameric DnaB helicase and its complex with a domain of DnaG primase. *Science* **318**, 459–463 (2007).
39. Lee, S.J. & Richardson, C.C. Interaction of adjacent primase domains within the hexameric gene 4 helicase-primase of bacteriophage T7. *Proc. Natl. Acad. Sci. USA* **99**, 12703–12708 (2002).
40. San Martin, M.C., Stamford, N.P.J., Dammerova, N., Dixon, N.E. & Carazo, J.M. A structural model for the *Escherichia coli* DnaB helicase based on electron microscopy data. *J. Struct. Biol.* **114**, 167–176 (1995).
41. Stamford, N.P.J., Lilley, P.E. & Dixon, N.E. Enriched sources of *Escherichia coli* replication proteins. The dnaG primase is a zinc metalloprotein. *Biochim. Biophys. Acta* **1132**, 17–25 (1992).
42. Wijffels, G. *et al.* Inhibition of protein interactions with the β_2 sliding clamp of *Escherichia coli* DNA polymerase III by peptides from β_2-binding proteins. *Biochemistry* **43**, 5661–5671 (2004).
43. Hamdan, S. *et al.* Hydrolysis of the 5′-*p*-nitrophenyl ester of TMP by the proofreading exonuclease (ε) subunit of *Escherichia coli* DNA polymerase III. *Biochemistry* **41**, 5266–5275 (2002).
44. Oakley, A.J. *et al.* Flexibility revealed by the 1.85 Å crystal structure of the β sliding-clamp subunit of *Escherichia coli* DNA polymerase III. *Acta Crystallogr. D Biol. Crystallogr.* **59**, 1192–1199 (2003).
45. Ozawa, K. *et al.* Cell-free protein synthesis in an autoinduction system for NMR studies of protein-protein interactions. *J. Biomol. NMR* **32**, 235–241 (2005).
46. Xiao, H., Crombie, R., Dong, Z., Onrust, R. & O'Donnell, M. DNA polymerase III accessory proteins. III. *holC* and *holD* encoding χ and ψ. *J. Biol. Chem.* **268**, 11773–11778 (1993).
47. Gulbis, J.M. *et al.* Crystal structure of the chi:psi sub-assembly of the *Escherichia coli* DNA polymerase clamp-loader complex. *Eur. J. Biochem.* **271**, 439–449 (2004).
48. Williams, N.K. *et al. In vivo* protein cyclization promoted by a circularly permuted *Synechocystis* sp. PCC6803 DnaB mini-intein. *J. Biol. Chem.* **277**, 7790–7798 (2002).
49. Maki, S. & Kornberg, A. DNA polymerase III holoenzyme of *Escherichia coli*. I. Purification and distinctive functions of subunits τ and γ, the *dnaZX* gene products. *J. Biol. Chem.* **263**, 6547–6554 (1988).
50. Pritchard, A.E., Dallmann, H.G., Glover, B.P. & McHenry, C.S. A novel assembly mechanism for the DNA polymerase III holoenzyme DnaX complex: association of δδ′ with $DnaX_4$ forms $DnaX_3$δδ′. *EMBO J.* **19**, 6536–6545 (2000).

Corrigendum: Single-molecule studies of fork dynamics in *Escherichia coli* DNA replication

Nathan A Tanner, Samir M Hamdan, Slobodan Jergic, Karin V Loscha, Patrick M Schaeffer, Nicholas E Dixon & Antoine M van Oijen

***Nat. Struct. Mol. Biol.* 15, 170–176 (2008); published online 27 January 2008; corrected after print 18 June 2008**

In the version of this article initially published, Karin V. Loscha was missing from the list of authors. The error has been corrected in the HTML and PDF versions of the article.